Tbx3 can alter limb position along the rostrocaudal axis of the developing embryo

Charalampos Rallis, Jo Del Buono and Malcolm P. O. Logan*

Division of Developmental Biology, National Institute for Medical Research, Mill Hill, London NW7 1AA, UK

*Author for correspondence (e-mail: mlogan@nimr.mrc.ac.uk)

Summary

The limbs of the vertebrate embryo form at precise locations along the body and these positions are fixed across different species. The mechanisms that control this process are not understood. Ectopic expression of *Tbx3*, a transcriptional repressor that belongs to the Tbx2/3/4/5 subfamily of T-box transcriptional regulators, in the forelimb results in a rostral shift in the position of the limb along the main body axis. By contrast, a transcriptional activator form of *Tbx3* shifts the limb to more caudal locations. We also show that *dHand* and *Gli3*, genes previously implicated in anteroposterior pre-patterning of the limb-forming region, are also involved in refining the position of the limbs. Our data suggest a new role for *Tbx3* in positioning the limb along the main body axis through a genetic interplay between *dHand* and *Gli3*.

Key words: Limb development, Limb position, *Tbx3*, T-box, *Gli3*, *dHand* (Hand2), Chick

Introduction

Vertebrate limbs develop as budding outgrowths from the lateral plate mesoderm (LPM) on either side of the main body axis. The forelimb and hindlimb fields are located at specific positions along the rostrocaudal axis of the embryo and this position is fixed across vertebrate species. The forelimb forms at the cervical-thoracic junction, while the hindlimb develops at the level of the lumbar-sacral junction (Burke et al., 1995). Hox genes are candidates to specify limb position. Many of these genes are expressed in nested patterns along the rostrocaudal axis of the embryo and may provide positional cues to cells of the LPM that will give rise to limb buds (Burke, 2000; Burke et al., 1995; Cohn et al., 1995; Cohn et al., 1997). However, neither gene deletion nor gene misexpression experiments have provided direct evidence for a role of Hox genes in limb positioning.

Tbx3 belongs to the Tbx2/3/4/5 subfamily of T-box genes that originated from a single ancestral gene through gene tandem duplication and cluster dispersion (Agulnik et al., 1996; Minguillon and Logan, 2003; Ruvinsky et al., 2000; Wilson and Conlon, 2002). *Tbx3* is expressed in the limb-forming territories prior to overt limb bud outgrowth. At later stages (st.24 chick, 11.5 dpc in the mouse), *Tbx3* is expressed in two stripes in the anterior and posterior limb mesenchyme (Gibson-Brown et al., 1998; Logan et al., 1998; Tumpel et al., 2002). *Tbx3* is required for normal limb development as mutations in human *TBX3* are associated with Ulnar-Mammary Syndrome (UMS, OMIM #181450), a dominant disorder characterized by upper(fore) limb deficiencies (Bamshad et al., 1997). Posterior structures of the limb, e.g. the ulna and fifth digit, are predominantly affected. *Tbx3* deletion studies in the mouse produce phenotypes consistent with the abnormalities observed in UMS (Davenport et al., 2003).

Experiments in the chick have shown that the posterior domain of *Tbx3* expression in the limb is positively regulated by *Shh* signalling, while the anterior expression domain is repressed by *Shh*, suggesting a potential role of *Tbx3* in the anteroposterior patterning of the vertebrate limb (Tumpel et al., 2002). Furthermore, recent misexpression experiments have suggested that *Tbx3* can alter the identity of posterior digits in the developing chick hindlimb (Suzuki et al., 2004).

Misexpression and gene deletion studies have implicated *Tbx3* in limb patterning during limb bud stages. However, *Tbx3* is expressed in the limb-forming region prior to overt limb bud outgrowth. To examine a potential early role of *Tbx3* in normal limb development, we have misexpressed transcriptional repressor and activator forms of *Tbx3* in the developing forelimb region using the avian retroviral system. We provide evidence for a new role for *Tbx3* in the genetic network that positions the limb along the rostrocaudal axis of the vertebrate embryo.

Materials and methods

Embryos

Eggs (Needle's farm, Winter's farm, The Poultry Farm) were incubated at 37°C and staged according to Hamburger-Hamilton (HH) (Hamburger and Hamilton, 1951).

Retrovirus production and embryo infection

Production of retroviral supernatants were carried out as described previously (Logan and Tabin, 1998). Two full-length *Tbx3* viruses were produced; one includes amino acid residues 1-732 the other amino acid 15-732 of the predicted protein (AF033669). Both forms produced identical results. *Tbx3^EN^* contains amino acids 15-289 of Tbx3, which spans the N terminus and DNA-binding T-domain, fused to the engrailed repressor domain (Jaynes and O'Farrell, 1991). *Tbx3^VP16^* contains the same residues fused to two VP16 activation

domains (Ohashi et al., 1994). The Gli3ZnF-Vp16 construct contains amino acids 471-636 of the human GLI3 (XP_004833) fused to two VP16 activation domains. The prospective forelimb territory on the right side of the embryo were infected between stages 8 and 10, as previously described (Logan and Tabin, 1998). The left limb served as a contralateral control. Each virus produced a limb shift phenotype in ~30% of infected embryos. For embryos analyzed before a limb shift phenotype was morphologically obvious, batches of infected embryos were analyzed. For embryos analyzed at later stages, embryos with a phenotype were selected.

Whole-mount in situ hybridization

Whole mount in situ hybridizations were carried out essentially as described (Riddle et al., 1993). Probes used were *Shh* (Riddle et al., 1993), *Fgf8* (Vogel et al., 1996), *MyoD, Pax3* (Pourquie et al., 1996), *Hoxb8, Hoxb9, Hoxc5, Hoxd12* (Burke et al., 1995), *Wnt26* (Kawakami et al., 2001), *Tbx5, Tbx2, Tbx3* (Logan et al., 1998), *dHand* (also known as *Hand2*) (Fernandez-Teran et al., 2000), *Gli3* (Schweitzer et al., 2000) and *Bmp2* (Schlange et al., 2002). The *Tbx15* probe was produced from a cDNA isolated from a limb cDNA library (M.P.O.L., unpublished).

Whole-mount immunohistochemistry

Whole-mount immunohistochemistry was performed as previously described (Kardon, 1998). Axons were stained using the 3A10 monoclonal antibody (hybridoma supernatant diluted 1/100 from DSHB, Iowa, USA) and detected with a peroxidase-conjugated anti-mouse secondary (Jackson ImmunoResearch) diluted 1/250.

Cell lines, transfections and luciferase assays

Luciferase assays were performed using COS1 cells. Transfections were performed using Superfect transfection reagent (Qiagen) following the manufacturer's protocol. For expression studies, full-length, Engrailed and VP16 fusion forms were cloned into pcDNA3.1(–) (Invitrogen). The reporter pGL3-promoter vector (Promega) containing a single *Brachyury* binding site (Kispert et al., 1995) together with a basal SV40 promoter upstream of the *Firefly* Luciferase gene. Luciferase assays were carried out using the appropriate Reporter Assay System (Promega) according to the manufacturer's protocol. Normalization of the results was carried out using β-Galactosidase Reporter Assay (Promega) according to the manufacturer's protocol. As an internal control the reporter plasmid was co-transfected with the β-galactosidase reporter only. All experiments were performed in triplicate. Error bars represent the standard deviation over three experiments.

DiI injection

DiI crystals (Sigma) were diluted in 100% ethanol (5 mg/ml). A 10% working solution was prepared in 30% sucrose/PBS solution. Misexpression of retrovirus was performed at HH stage 8-10. Twenty-four hours after retrovirus infection (stage 14) DiI solution was injected into the embryos at several levels in the limb-forming region of the LPM and in the adjacent somites, to serve as axial reference. Equivalent DiI injections were performed in the injected and control side of the embryo.

Results

Analysis of *Tbx3* expression in the developing chick embryo

To analyse the expression pattern of *Tbx3* at stages prior to limb outgrowth, we performed whole-mount in situ hybridization between stages 12-16. *Tbx3* expression is observed in the future forelimb and hindlimb domains at stages 12-13 (Fig. 1A), earlier than previously reported (Tumpel et al., 2002). Just prior to overt limb outgrowth (stage 16), *Tbx3*

is expressed in the presumptive forelimb and hindlimb areas (Fig. 1B) and expression appears more robust in the posterior region (Fig. 1B). In situ hybridization on sections of the forelimb region of stage 16 embryos (Fig. 1C,D) reveals that *Tbx3* is present in the mesoderm of the presumptive wing region and in the lateral lip of dermomyotome. At stage 19, when a limb bud is clearly evident, expression is prominent in the posterior of the limb (Fig. 1E). At later stages (stage 25), expression is located in two stripes in the anterior and posterior limb mesenchyme (Fig. 1F).

Tbx3 is a transcriptional repressor *in vitro*

In vitro data suggest that human *TBX3* is a transcriptional repressor (Carlson et al., 2001). We generated three constructs:
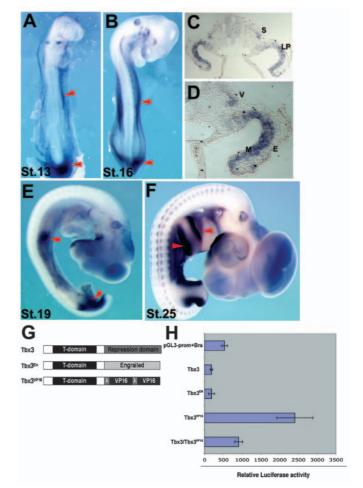

Fig. 1. Normal expression of *Tbx3* in the chick (A-F). (A) At stage13, *Tbx3* is expressed in the presumptive forelimb (FL) and hindlimb (HL) levels (arrowheads). (B) At stage 16, *Tbx3* expression is more robust in the posterior of the limb (arrowheads). (C) Stage16 section at the forelimb level. *Tbx3* is expressed in the lateral plate mesoderm and somite. (D) Higher magnification of section in C. *Tbx3* is present in the mesoderm but not ectoderm of the wing and in the ventrolateral lip of the dermomyotome. (E) Stage 19, *Tbx3* is located in the posterior limb mesenchyme (arrowheads). (F) Stage 25, *Tbx3* is present in the limbs in two stripes in the anterior and posterior limb mesenchyme (arrowheads). (G) Schematic diagrams of *Tbx3* constructs. (H) Bar chart representing the relative luciferase activity obtained in luciferase assays with *Tbx3* constructs. S, somite; LP, lateral plate mesoderm; V, ventral lip of dermomyotome; M, mesoderm; E, ectoderm.

full-length Tbx3 (Tbx3); a construct that contains the N-terminus and T-domain of Tbx3 fused to the VP16 transcriptional activator domain (Ohashi et al., 1994) (Tbx3^{VP16}); and a construct with the same residues fused directly to the repressor domain of the *Drosophila engrailed* gene (Jaynes and O'Farrell, 1991) (Tbx3^{EN}) (Fig. 1G, see Materials and methods). The Tbx3^{VP16} construct is predicted to compete with endogenous Tbx3 protein for binding sites and activate target genes. The Tbx3 and Tbx3^{EN} forms are predicted to repress target genes. Engrailed repressor activity is Groucho dependent (Jimenez et al., 1997) and Groucho homologues are present in the limb mesenchyme (Rallis et al., 2003). To test the transcriptional properties of these three Tbx3 constructs, we performed in vitro luciferase assays using a reporter plasmid containing a single T-box binding site. Both Tbx3 and Tbx3^{EN} fusion constructs repress expression to an almost equal extent. By contrast, the Tbx3^{VP16} fusion construct activates expression (Fig. 1H). Co-transfection of Tbx3/Tbx3^{VP16} generates luciferase activity at intermediate levels between those achieved with Tbx3 or Tbx3^{VP16} alone. Together, the data demonstrate that Tbx3 functions as a transcriptional repressor in vitro.

Misexpression of *Tbx3* can alter limb position

We have investigated the role of *Tbx3* in normal limb development using the chicken retroviral system. Following our targeting strategy (Materials and methods), we could detect virus broadly in the limb-forming region from stage 14 onwards (data not shown). Strikingly, misexpression of full-length *Tbx3* shifted the axial position of the injected limb rostrally (embryos that show rostral limb shift phenotype: *n*=142; phenotype frequency 25-30%). Identical results were produced with *Tbx3^{EN}* (embryos with phenotype; *n*=82, phenotype frequency 25-30%), further suggesting that Tbx3 normally functions as a transcriptional repressor. Comparison with *MyoD*, which is expressed in the dermomyotomal compartment of each somite and serves as an axial reference, and *Shh*, which marks the zone of polarizing activity (ZPA) in the posterior limb, demonstrates the rostral shift in limb position following *Tbx3* misexpression (limb on right), relative to contralateral control limbs (on left in all cases shown) (Fig. 2A, *n*=6/6, 100%). The shift in axial position can extend over the distance of one to three somites; however, the limb itself is otherwise morphologically normal. *Pax3* is expressed in the dermomyotome of the developing somites and the migrating myoblasts (Williams and Ordahl, 1994). Following misexpression of *Tbx3* and mislocation of the limb to a more rostral position along the embryo axis, myoblasts that migrate into the shifted limb are derived from somites at a more rostral level. Myoblasts at more caudal levels that normally migrate into the limb (Fig. 2B, black arrow), no longer contribute to the limb musculature and remain within the dermomyotome (Fig. 2B, red arrow) (*n*=7/7, 100%). Both delamination and migration of the myoblasts into the limb depend on the Met receptor and its ligand HGF, also called scatter factor, produced by non-somitic mesoderm (Dietrich et al., 1999). Following shift of the limb from its normal position, the source of HGF is presumably also shifted, leading to migration of myoblasts from somites at the incorrect axial level.

The neurons that innervate the wing and form the brachial plexus originate from the 16th to 19th spinal ganglia (Lillie,
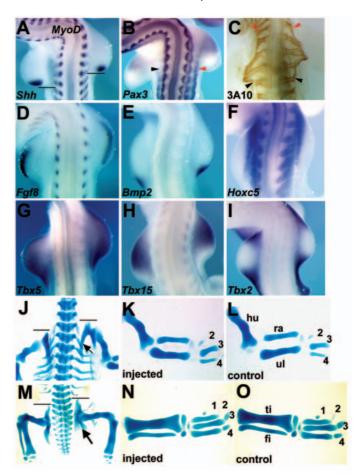

Fig. 2. Misexpression of *Tbx3* and *Tbx3^{EN}* causes a rostral shift in limb position but the shifted limb is patterned normally. Dorsal views of embryos; injected side is on the right, control side is on the left. Rostral is towards the top. (A) Whole-mount in situ hybridization with *MyoD* marking somites and *Shh* marking the ZPA. There is a one somite-level shift in limb position (compare level of left and right bar). (B) Whole-mount in situ hybridization with *Pax3* marking migrating myoblasts from the lateral lip of dermomyotome into the limb mesenchyme. *Pax3* is not detected in the lateral lip of the dermomyotome in somites at levels that normally contribute to limb musculature (black arrowhead), as these cells have migrated into the limb. Following a limb shift on the injected side, these *Pax3*-expresssing cells are still present in somites at the same axial level (red arrowhead). (C) Whole-mount immunohistochemistry for the neurofilament-associated antigen (3A10). Axons from axial levels that normally innervate the limb fail to send projections to the shifted limb (right, black arrowheads). At more rostral levels, following mislocation of the limb, axons that normally do not innervate the limb on the injected side, project into the limb mesenchyme (red arrowheads). (D-I) Genes expressed in regions of the limb ectoderm or mesenchyme. *Fgf8* (D), *Bmp2* (E), *Hoxc5* (F), *Tbx5* (G), *Tbx15* (H) and *Tbx2* (I) are all expressed in their normal pattern in the shifted limb. (J-O) Skeletal preparations of an embryo injected with *Tbx3* in the wing (J-L) or in the leg (M-O). Although the wing and the leg are shifted rostrally (compare bar levels between left and right side in J and M), no alterations are observed in the vertebral column. Arrow in J indicates scapula, arrow in M indicates ischium. (K) Injected wing; (L) contralateral control wing. There is no alteration in the pattern of the limb elements. (N) Injected leg; (O) uninjected leg. No change is observed in digit patterning following *Tbx3* misexpression. Chick stages: (A) 22, (B) 23, (C) 24, (D-I) 21, (J-O) 27.

1927). Transplantation of a limb to the interlimb region results in the migration of neuron axons from the spine into the ectopic limb from axial levels that normally do not contribute to limb innervation (Hamburger, 1939). Consistent with transplantation studies the shifted limb is innervated by neurons from the 15th to 18th spinal ganglia (Fig. 2C, *n*=6/6). Therefore, following rostral shift of the limb, neuron axons that normally would not participate in innervation of the wing, are recruited into the limb (Fig. 2C, red arrows) and axons that would normally enter the limb mesenchyme no longer do so (Fig. 2C, black arrows). Therefore, following the mislocation of the limb to a more rostral position, several cell-types undergo changes in their developmental program and contribute to different regions of the body.

The limb shifted by *Tbx3* misexpression is patterned normally

In a previous study, misexpression of *Tbx3* and *Tbx2* in the developing hindlimb, results in changes in anteroposterior patterning of digits, suggesting these genes have a role in specifying digit identity (Suzuki et al., 2004). To determine if patterning of the shifted limb is altered following our misexpression strategy, we analyzed the expression of genes normally regionally restricted within the limb. *Fgf8* is expressed in the AER of the injected wing in a pattern indistinguishable from the control limb (Fig. 2D; *n*=5/5, 100%). *Bmp2*, which is expressed in the AER and in the posterior of the limb as a response to Shh signalling (Francis et al., 1994), is expressed in an identical pattern in injected and uninjected limbs (Fig. 2E; *n*=5/5, 100%) in contrast to other reports (Suzuki et al., 2004). This is consistent with the normal distribution of *Shh* in *Tbx3*-injected limbs (Fig. 2A). *Hoxc5*, which is normally expressed in proximal regions of the limb mesenchyme (Burke et al., 1995), is unaffected in the injected limb (Fig. 2F; *n*=6/6, 100%). Expression of other T-box genes is also unaffected within the shifted limb despite the rostral mislocation: *Tbx5* is expressed throughout the limb mesenchyme (Fig. 2G; *n*=7/7, 100%); *Tbx15* is expressed in medial regions of the limb (Fig. 2H; *n*=6/6, 100%); and *Tbx2* is expressed in anterior and posterior stripes, in a similar pattern to *Tbx3* (Fig. 2I; *n*=6/6, 100% compare with Fig. 1H).

We also analyzed skeletal preparations of embryos with a shift phenotype that were allowed to develop to later stages (stage 27). In these examples, the vertebral column of the embryo is normal. However, the limb skeletal elements, including the scapula are mislocated rostrally, although there is no alteration in their morphology (Fig. 2J, *n*=10/10, 100%). Moreover, the morphology of the digits in the shifted wing (Fig. 2K) is normal compared with those in the contralateral control limb (Fig. 2L). No alterations in digit identity were observed. The same results were obtained following misexpression of *Tbx3* in the developing hindlimbs (Fig. 2M; *n*=10/10, 100%). The axial position of the injected limb is shifted rostrally along the rostrocaudal axis, but hindlimb digit morphology (Fig. 2N) is indistinguishable from that in the contralateral control leg (Fig. 2O). In *Tbx3*-injected embryos with a shifted wing (*n*=8) or leg (*n*=7) analyzed at stage 27, *Sox9* expression, which marks the skeletal progenitors, is normal in both forelimbs and hindlimbs, confirming the results obtained from skeletal preparations (data not shown).

Axial Hox gene expression is unaffected following *Tbx3* misexpression

To understand the mechanism underlying the rostral shift in limb position, we investigated the effects of *Tbx3* misexpression at stages prior to morphological limb shifts (stage 13-16). Following our retroviral targeting strategy, by stage 13, transcripts for *Tbx3* are detected at normal levels on the injected side (right) (Fig. 3A; 15/15, 100%). By stage 16, transcripts are present throughout the limb-forming territory on the injected side, while on the uninjected side they are restricted to the posterior (Fig. 3B; 2/12, 17%). Although there is no direct evidence that axial Hox gene expression controls the position of the limb primordia, the axial position at which the limbs develop correlates with the expression of several Hox genes in the LPM (Burke, 2000; Burke et al., 1995; Cohn et
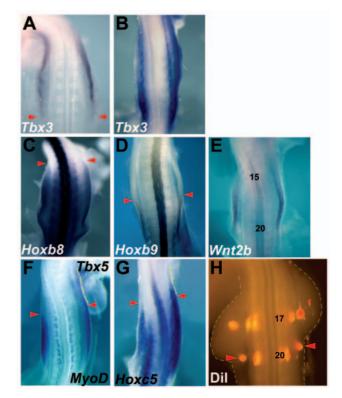

Fig. 3. Early effects of *Tbx3* misexpression at the forelimb level. In all panels, injected side is rightwards and control side is leftwards. Rostral is towards the top. (A) Levels of *Tbx3* transcripts are unaffected at stage 13. (B) By stage 16, *Tbx3* transcripts are detected throughout the limb field on the injected side. (C,D) There is no alteration in the rostral border (red arrowheads) of *Hoxb8* (C) or *Hoxb9* (D) following misexpression of *Tbx3*. (E) *Wnt2b* is expressed normally in the early forelimb-forming territory. The limb-forming region extends between somites 15 and 20 (numbered). (F) *Tbx5* expression is expanded rostrally. The extent of rostral expansion is indicated with a broken yellow line. Red arrowheads indicate equivalent rostrocaudal levels. (G) Rostral expansion of *Hoxc5* expression (indicated with a broken yellow line). Red arrowheads show equivalent rostrocaudal levels. (H). DiI labelling of the prospective limb-forming region and adjacent somites (for axial reference). In the uninjected limb, cells that normally contribute to the posterior limb stay in register with somites at the same axial level (left, arrowhead). On the injected side (right), cells at the same level instead contribute to the inter-limb flank but remain in register with adjacent somites (arrowhead). Somites 17 and 20 are numbered.

al., 1995; Cohn et al., 1997; Rancourt et al., 1995). Axial Hox gene expression is not altered in the *Tbx3*-injected forelimb area. The rostral expression boundary of *Hoxb8* is not changed (Fig. 3C; *n*=30/30, 100%). In addition, the expression boundary of *Hoxb9,* which is caudal to the region of the LPM that will give rise to the posterior forelimb mesenchyme (Burke et al., 1995; Cohn et al., 1997), is at the same level on the rostrocaudal axis of the embryo in both the control and injected side (Fig. 3D; *n*=27/27, 100%). Further analysis of the expression of several other Hox genes (*Hoxb4*, *Hoxc4*, *Hoxb5*, *Hoxc6*, *Hoxa9*, *Hoxc9* and *Hoxd9*) produced identical results (data not shown). These results indicate that the mechanism that shifts limb position in *Tbx3*-injected embryos lies downstream of any axial Hox code that may act to position the limbs.

Effects of *Tbx3* misexpression on limb mesenchyme markers

Experiments in the mouse, chick and zebrafish have established that *Tbx5* is required for forelimb initiation (Agarwal et al., 2003; Ahn et al., 2002; Ng et al., 2002; Rallis et al., 2003; Takeuchi et al., 2003). The secreted factor *Wnt2b* has also been implicated in limb initiation (Kawakami et al., 2001). Experiments in zebrafish have suggested that *wnt2b* acts upstream of *tbx5* during forelimb initiation (Ng et al., 2002). Following misexpression of repressor forms of Tbx3, the domain of *Wnt2b* expression is unaffected (Fig. 3E; *n*=27/27, 100%); however, the domain of *Tbx5* expression is expanded to more rostral regions of the LPM, whereas the more caudal expression domain, which would normally give rise to the posterior limb mesenchyme, is initially unaffected (Fig. 3F; *n*=6/19, 32%). These results would suggest that the effects of *Tbx3* are mediated downstream or in parallel with *Wnt2b*. Expression of *Hoxc5*, which is also expressed in the early limb bud mesenchyme, is also expanded rostrally (Fig. 3G; *n*=7/20, 35%). These data demonstrate that the rostral shift in the limb is preceded by a rostral expansion of the limb mesenchyme, while their caudal domain is unchanged. At later stages, however, the expression domains of *Hoxc5* and *Tbx5* within the limbs are shifted rostrally (Fig. 2F,G). At this stage, *Shh* expression is not expanded but is present in a more rostral domain (Fig. 2A). In conclusion, after misexpression of *Tbx3*, there is an initial rostral expansion of the limb-forming region that is followed by a subsequent shift in axial limb position.

To investigate whether cell movement accounts for the phenotype, we performed DiI labelling experiments to follow the fates of cells of the prospective limb-forming region. Following misexpression of *Tbx3*, cells that normally become part of the posterior limb mesenchyme are instead incorporated into the interlimb flank (Fig. 3H; *n*=5/5, 100%). Cells in more rostral locations that would not normally contribute to the limb, are recruited to form (anterior) limb. Therefore, the shift in limb position cannot be attributed to migration of cells in the LPM.

Tbx3 and positioning of the ZPA

A shift in limb position is demonstrated by the expression of *Shh*, in the posterior of the limb bud, at an inappropriate axial level (Fig. 2A). We therefore examined the expression of *dHand* and *Gli3*, genes which are involved in pre-patterning the anteroposterior axis of the limb and establishing the position of *Shh* expression in the ZPA (Charite et al., 2000; Fernandez-Teran et al., 2000; te Welscher et al., 2002). During limb induction stages, *dHand* (also known as *Hand2*), a bHLH

transcription factor, is expressed throughout the limb-forming region (Fig. 4A) (Charite et al., 2000; Fernandez-Teran et al., 2000). Subsequently, *Gli3*, a zinc-finger transcription factor, is expressed throughout almost the entire limb mesenchyme in an anterior-to-posterior graded fashion (Schweitzer et al., 2000). Genetic antagonism between *Gli3* and *dHand* results in downregulation of *dHand* expression in the anterior limb mesenchyme (Fig. 4B). At later stages, *dHand* and *Gli3* are expressed in the anterior and posterior limb mesenchyme, respectively, with an overlapping domain of co-expression in the medial limb (Fig. 4C). The interactions between *dHand* and *Gli3* ultimately position the ZPA prior to *Shh* signalling (te Welscher et al., 2002; Zuniga and Zeller, 1999). Following misexpression of *Tbx3*, *dHand* is expressed throughout the limb-forming region, while in the control side *dHand* is restricted to the posterior limb mesenchyme (Fig. 4D; *n*=7/22, 32%). In addition, there is a downregulation of *Gli3* throughout the injected limb and the caudal border of its graded expression domain shifts rostrally (Fig. 4G; *n*=8/22, 36%). At slightly later stages (stage 19), when the shift phenotype is already apparent, the domain of *dHand* expression is shifted to a more rostral location and is no longer expressed throughout the limb mesenchyme but is restricted to the posterior (Fig. 4E; *n*=7/7, 100%). Similarly, at stage 19, *Gli3* is expressed in more rostral locations, in an anterior-posterior gradient in the limb mesenchyme of the shifted limb (Fig. 4H; *n*=8/8, 100%). At later stages (stage 21) when the shift phenotype is obvious, *dHand* is expressed normally in the posterior mesenchyme of the shifted limb (Fig. 4F; *n*=7/7, 100%) and *Gli3* has a normal distribution in the anterior mesenchyme (Fig. 4I; *n*=8/8, 100%). To more accurately define the time course of the limb shift phenotype, we also analyzed expression of *Shh* and a downstream target of *Shh*, *Hoxd12*, in *Tbx3*-injected limbs at stage 19. Expression domains of both *Shh* (Fig. 4J, *n*=2/2, 100%) and *Hoxd12* (Fig. 4L; *n*=2/2, 100%) were shifted to more rostral positions. At later stages (stage 21), *Shh* (Fig. 4K, *n*=2/2, 100%) and *Hoxd12* (Fig. 4M; *n*=2/2, 100%) were expressed in the normal, posterior domains within the shifted limb. These data show that following misexpression of *Tbx3*, the normal restriction of *dHand* expression to the posterior limb mesenchyme and *Gli3* to anterior is initially disrupted at early limb-forming stages prior to *Shh* expression. However, as soon as *Shh* is detectable, its expression domain is shifted to more rostral locations. The establishment of this altered expression domain serves as the first molecular evidence of a shift in the rostrocaudal location of the limb. After limb position has shifted, *dHand* and *Gli3* expression is normal within the limb mesenchyme.

Misexpression of Tbx3[VP16] can shift the limb caudally in axial position

As a complementary approach to misexpressing *Tbx3* and *Tbx3[EN]*, we misexpressed *Tbx3[VP16]* in the presumptive forelimb area. In contrast to *Tbx3* and *Tbx3[EN]*, which act as repressors, *Tbx3[VP16]* behaves as a transcriptional activator (Fig. 1F). Moreover, Tbx3[VP16] has the ability to interfere with the repressor activity of Tbx3 in our *in vitro* luciferase system (Fig. 1F). We predict that Tbx3[VP16] is able to compete with endogenous Tbx3 for binding sites, and targets will be activated instead of repressed. Following misexpression of Tbx3[VP16], the injected limb is displaced caudally in axial
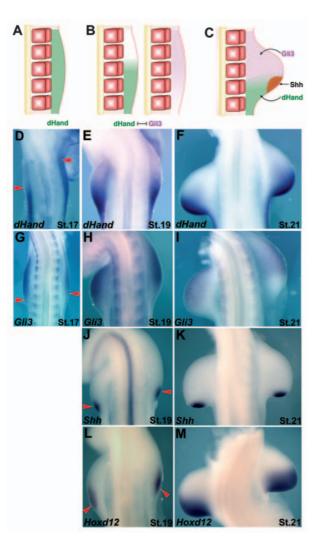
Development

Fig. 4. Effects of *Tbx3* and *Tbx3^EN* misexpression on *dHand* and *Gli3* expression. (A-C) Schematics of the limb-forming region. (A) At stage 16, *dHand* is present throughout the limb forming region. (B) At stage 17, high levels of *dHand* expression are observed in the posterior limb mesenchyme owing to repression by *Gli3*, which is expressed at higher levels in the anterior. (C) At stage 18, *Gli3* is expressed in the anterior limb mesenchyme, while *dHand* in the posterior is required for the establishment of *Shh* expression in the ZPA. In medial limb mesenchyme, *dHand* and *Gli3* expression domains overlap. (D) At stage 17, *dHand* is restricted in the posterior limb mesenchyme in the control side (left, arrowhead shows rostral border of expression). Following *Tbx3* misexpression, dHand is expressed throughout the limb-forming region (right, arrowhead). At stage 19 (E) and stage 21 (F), when the alteration in limb position is apparent, normal expression of *dHand* is observed within the limb mesenchyme of the shifted limb. (G) At stage 17, following *Tbx3* misexpression, *Gli3* is downregulated in the injected side (right arrowhead) compared with the control side (left arrowhead). A rostral shift in the graded *Gli3* expression domain is observed (compare left and right arrowhead levels). At stage 19 (H) and at later stages (stage 21) (I), *Gli3* is expressed normally within the mesenchyme of the shifted limb. *Shh* expressed in cells of the ZPA in the posterior of the limb is detected in more rostral locations in the shifted limb by stage 19 (J) and also at stage 21 (K). *Hoxd12*, a downstream target of *Shh*, is similarly expressed in more rostral locations in the *Tbx3*-injected limb by stage 19 (L) and also at stage 21 (M).
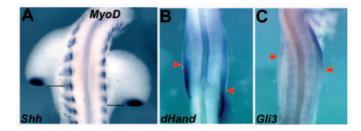

Fig. 5. Misexpression of Tbx3^VP16 causes a caudal shift in axial limb position. (A) *MyoD* expression marks the somites and *Shh* marks the ZPA. There is a two-somite level caudal shift (marked by bars) in the injected limb (right). (B) *dHand* expression at stage 17 following Tbx3^VP16 misexpression. *dHand* is restricted to the posterior limb mesenchyme in the control side (left, arrowhead shows rostral expression border), while in the injected side, *dHand* expression is displaced caudally (right, arrowhead). (C) *Gli3* expression at stage 17 following Tbx3^VP16 misexpression. *Gli3* is upregulated in the injected side (right) compared with the control side (left). The graded domain of *Gli3* expression is displaced caudally (compare left and right arrowheads).

position (embryos that show caudal limb shift phenotype *n*=42; frequency of phenotype 30%). In situ hybridization for *MyoD* and *Shh* demonstrates the caudal shift in axial position (Fig. 5A, *n*=7/7, 100%). The limb displacement can extend over the distance of one to three somites but, as with rostral limb shifts, the limb itself is otherwise normal. We examined the expression of *dHand* and *Gli3* at pre-limb bud stages, following misexpression of *Tbx3^VP16*. Although in the control, *dHand* expression is restricted to posterior mesenchyme of the limb, following misexpression of *Tbx3^VP16*, there is a caudal displacement of the expression domain of *dHand* (Fig. 5B, *n*=9/30, 33%). In addition, there is an upregulation of *Gli3* expression (Fig. 5C, *n*=8/25, 32%). These results show that by misexpressing *Tbx3^VP16*, we are able to generate a limb shift in the opposite direction to that obtained using *Tbx3* and *Tbx3^EN*. The data also suggest that *Tbx3* acts as a transcriptional repressor in the limb bud.

Gli3 is implicated in positioning the limb

Following misexpression of *Tbx3*, *Gli3* mRNA levels are decreased within the limb mesenchyme and the caudal border of its expression is shifted rostrally (Fig. 4G). Gli3 is a bifunctional zinc-finger transcription factor that undergoes default proteolysis to a truncated form (Gli3^R) that represses expression of *Shh* target genes. In the presence of Shh signalling, processing to produce the Gli3^R form is blocked and a full-length Gli3 protein is formed. Contradictory data, generated both in vitro and in vivo, suggest that the full-length Gli3 molecule is either an activator or a repressor (Bai et al., 2004; Litingtung et al., 2002; Sasaki et al., 1997; Wang et al., 2000). The effect of *Tbx3* misexpression on *Gli3* is observed at stages prior to *Shh* expression when Gli3 is acting as a repressor. To investigate whether *Gli3* can directly alter limb positioning, we misexpressed a form of Gli3 that contains the DNA-binding domain of the protein fused with two VP16 activation domains (Gli3ZnF-VP16, Fig. 6A). Gli3ZnF-VP16 has the ability to bind Gli3 binding sites and activate transcription (D. Stamataki, F. Ulloa and J. Briscoe, personal communication). Misexpression of this form of Gli3 is

predicted to compete with the endogenous Gli3 repressor (Gli^R) for binding sites and to activate, rather than repress, target genes and thereby lower the repressor activity of endogenous Gli3. Misexpression of Gli3ZnF-VP16 generated a phenotypically similar result to that obtained following misexpression of Tbx3 repressor forms (embryos that show the rostral limb shift phenotype *n*=48; phenotype frequency 35-40%). A rostral shift in axial limb position is evident by comparing *MyoD* and *Shh* expression domains (Fig. 6B, *n*=7/7, 100%) and can extend from one to three somites. Following misexpression of Gli3ZnF-VP16, the *Tbx3* expression domain is expanded rostrally in the injected side compared with the contralateral control side (Fig. 6C, *n*=6/16, 38%). A similar expansion is observed in *dHand* expression (Fig. 6D, *n*=5/14, 36%). By contrast, the endogenous expression of *Gli3* is decreased following misexpression of Gli3ZnF-VP16 (Fig. 6E, *n*=5/13, 38%). These results suggest that *Gli3* is a candidate to play a role in positioning the limb field and may do so through a genetic interaction between *dHand* and *Tbx3*.

Discussion

Tbx3 is a transcriptional repressor participating in mechanisms that position the limb

Our results, and those of others, demonstrate that Tbx3 can act as a transcriptional repressor in vitro (Fig. 1) (Carlson et al., 2001). Consistent with these observations, misexpression of *Tbx3* and *Tbx3^{EN}* in the forelimb region produces identical phenotypes, while misexpression of *Tbx3^{VP16}* generates the opposite phenotype. Data from in vitro and in vivo experiments suggest that Tbx3 acts as a transcriptional repressor in the developing limb bud.

Following misexpression of *Tbx3*, the expression domains of genes expressed in the limb are initially expanded rostrally and this is followed by a shift in limb position. Cells of the flank, rostral to the limb, which would not normally contribute to the limb, now become incorporated into the limb. Furthermore, cells that normally form posterior limb mesenchyme now no longer contribute to the limb. Strikingly, these cells had presumably initially expressed *Tbx5*, a gene required and apparently sufficient for limb initiation (Agarwal et al., 2003; Ahn et al., 2002; Ng et al., 2002; Rallis et al., 2003; Takeuchi et al., 2003). Fate mapping shows that the altered contribution to the limbs is not simply explained by migration of limb bud precursors. Our data suggest that once a ZPA is established in a more rostral position, the positive feedback loop between ZPA and AER now operates at altered axial levels and the limb develops in an ectopic site. Noticeably, the size of the ectopic limb is the same as that of the normal limb, suggesting that a mechanism, yet to be determined, is functioning to regulate limb size.

Other members of the T-box gene family can influence the extent of the limb. *Tbx18* is expressed in lateral plate mesoderm as the limb buds form and the anterior limit of *Tbx18* expression coincides with the anterior border of the limbs. Following misexpression of *Tbx18* in the presumptive wing bud region, the anterior extent of the limb is expanded (Tanaka and Tickle, 2004). The wing bud is extended rather than shifted in position and this extension is only transient. At later stages, the limb appears to regulate its size and develops normally. *Brachyury* is expressed in the LPM at the onset of limb
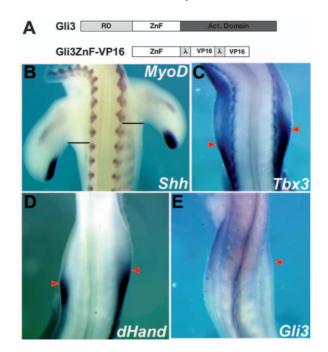

Fig. 6. Misexpression of a Gli3ZnF-VP16 activator form of *Gli3* can influence limb positioning. (A) Schematic of full-length Gli3 protein (Gli3) and a Gli3ZnF-VP16 activator form. Full-length Gli3 protein contains an N-terminal repression domain (RD), a zinc finger DNA-binding domain (ZnF), and an activation domain in the C-terminus (Act. Domain). The Gli3 activator form contains the ZnF fused with two VP16 activation domains. (B-E) Dorsal views of the embryo; injected limb is on the right. (B) Whole-mount in situ hybridization with *MyoD* indicates the somites and *Shh* marks the ZPA. There is a one-somite level shift in limb position (compare level of left and right bars) following misexpression of Gli3ZnF-VP16 in the limb. (C) The anterior border of the *Tbx3* (C) and *dHand* (D) expression domains in the forelimb region at stage 17 have been displaced rostrally (arrowheads) following Gli3ZnF-VP16 misexpression. (E) *Gli3* expression is downregulated following misexpression of Gli3ZnF-VP16 (arrowhead).

formation and at later stages of limb development, in the distal limb mesenchyme that lies underneath the AER. Misexpression of *Brachyury* in the chick wing results in anterior expansion of the AER and produces limb phenotypes consistent with augmented AER extent and function, including anterior digit duplications and, in rare cases, thickening of the anterior-most metatarsal (Liu et al., 2003).

Tbx3 misexpression does not affect the pattern of axial Hox gene expression. Hox genes have been implicated in limb position (Cohn et al., 1997) and a role for Hox genes in limb positioning is supported by *Hoxb5* knockout mice, which exhibit a unilateral or bilateral rostral shift in axial forelimb position (Rancourt et al., 1995). However, the phenotype in *Hoxb5$^{-/-}$* mice differs in several aspects from that obtained with *Tbx3* or *Tbx3^{EN}* misexpression. In *Hoxb5$^{-/-}$* mice, homeotic transformations of the cervico-thoracic vertebrae from C6-T1 are observed. The clavicle retains a medial articulation with its normal target, the sternum, resulting in a V-shaped shoulder girdle. The alteration in limb position in the *Hoxb5$^{-/-}$* mice is therefore associated with a transformation of the entire axial skeleton. The absence of an effect of *Tbx3* on the expression
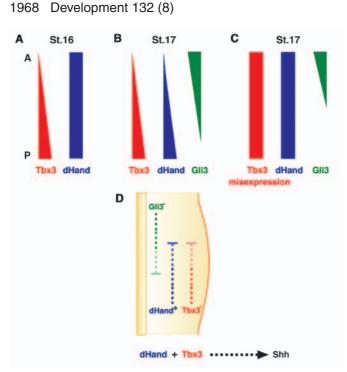
Fig. 7. Models for the interactions between *dHand*, *Gli3* and *Tbx3*, in the limb-forming region at stages prior to *Shh* expression, that refine limb position along the rostrocaudal axis of the embryo. (A) At stage 16, *Tbx3* is expressed throughout the limb-forming region but expression is more robust in the future posterior limb mesenchyme. *dHand* is expressed throughout the limb-forming region. (B) At stage 17, *Gli3* is expressed throughout the limb mesenchyme with higher levels in the anterior. *dHand* expression is restricted to the posterior. (C) Ectopic expression of *Tbx3* in more anterior regions leads to a repression of *Gli3*, resulting in a de-repression of *dHand* and expansion of its expression domain. (D) A model illustrating how the genetic antagonism between *dHand* and *Gli3* that positions the future ZPA may be mediated through *Tbx3*. – and + symbols indicate, respectively, the transcriptional repressor and activator function of each protein. In addition, in the posterior limb, *Tbx3* and *dHand* co-operate to induce *Shh* expression and thereby specify the position of the ZPA in the posterior limb mesenchyme. A, anterior; P, posterior.

of Hox genes indicates that *Tbx3* mediates its effects on limb position independently of any axial Hox code.

Normal limb patterning following misexpression of *Tbx3* forms

Roles for *Tbx3* and the related gene *Tbx2* in specifying posterior digit identity via *Shh* and *Bmp* signalling has been suggested (Suzuki et al., 2004; Tumpel et al., 2002). Our data implicate *Tbx3* in positioning the nascent limb at pre-bud stages, prior to *Shh* expression. However, we also analyzed the shifted limb at later stages. Following misexpression of full-length *Tbx3* and Tbx3EN, the expression pattern of *Bmp2* is unaffected, not expanded, as seen by Suzuki et al., and ultimately digit identity is unchanged. We also performed injections of *Tbx3* in the hindlimb-forming region and obtained the same result as seen in forelimbs: the injected hindlimb is shifted rostrally, while the digit array is unaffected, in contrast to previous results. Our results do not support a role for *Tbx3* in specifying digit identity. One difference between our experiments and those of Suzuki et al. is the timing of the viral

injections: while we performed our injections at stage 8-10, Suzuki et al. injected at stage 11-12. Our earlier stage misexpression protocol may account for our ability to generate limb shifts that were not reported by Suzuki et al. However, it is not clear why different effects on limb patterning were observed in these two sets of experiments, as our injection strategy does lead to broad ectopic expression of *Tbx3* at limb bud stages (Fig. 3B).

A genetic interplay between *Tbx3*, *dHand* and *Gli3*

At limb development stages, prior to *Shh* expression, genetic antagonism between *dHand* and *Gli3* establishes an anteroposterior pre-pattern of the limb that is ultimately responsible for establishing the position of the ZPA in the posterior limb. At these stages, *Gli3* is acting as a repressor (Wang et al., 2000), while *dHand* is shown to be a transcriptional activator (Dai and Cserjesi, 2002; Dai et al., 2002). Misexpression of *Tbx3* leads to an expansion, or failure of repression, of *dHand*, potentially through an interaction between *Tbx3* and *Gli3* (Fig. 7). We predict that *Tbx3* is acting to repress *Gli3* expression in the future posterior limb mesenchyme. Repression by *Tbx3* could be responsible for generating the anterior-to-posterior graded expression of *Gli3* in the developing limb primordium. This model is consistent with the observation that in *Tbx3* mutant mice, *dHand* is downregulated in the forelimbs and absent in the hindlimbs, which subsequently leads to a disruption in *Shh* expression. Our model would predict that downregulation of *dHand* is due to high *Gli3* expression that, in the absence of *Tbx3*, is no longer restricted to the anterior limb and expands to the posterior.

Misexpression of *Tbx3VP16* produces the opposite phenotype to that obtained with *Tbx3* and *Tbx3EN*; the limb shifts to a more caudal position than normal. *Gli3* expression is upregulated and expanded caudally in the *Tbx3VP16*-injected limbs, lending further support to a model in which *Tbx3* normally functions to restrict *Gli3* to the anterior mesenchyme. As a consequence of this *Gli3* expansion, the *dHand* expression domain is shifted caudally. By contrast, in *Tbx3*- and *Tbx3EN*-injected embryos, disruption of the normal repression of *dHand* by *Gli3* resets the rostrocaudal position of the ZPA to a more rostral position and this ultimately results in the limb shift phenotype. In *Tbx3VP16*-injected embryos, de-repression of *Gli3* shifts the expression domain of *dHand* and this ultimately leads to the ZPA forming more caudally. Our data demonstrate that the signals required for pre-patterning the AP axis of the limb and setting the position of the ZPA can influence the position of the limb along the rostrocaudal axis of the embryo.

Gli3 and limb positioning

We predict that the effects of Gli3ZnF-VP16 on *dHand* and *Tbx3* are caused by a disruption of endogenous GliR activity. Misexpression of Gli3ZnF-VP16 leads to the expansion of *Tbx3* and *dHand* expression domains, rather than the induction of ectopic patches of expression. This may indicate a non-cell autonomous action of *Gli3* on *dHand* and presumably also on *Tbx3*. A regulatory relationship between *Gli3* and *Tbx3* has been demonstrated during lung organogenesis (Li et al., 2004). *Tbx3* is normally expressed in the mouse lung in the presence of *Shh*. In this environment, *Gli3* acts as an activator of *Tbx3* transcription. In *Shh−/−* animals, where *Gli3* acts as a repressor,

Tbx3 transcripts are significantly reduced. However, in *Shh*$^{-/-}$/*Gli3*$^{-/-}$ animals, de-repression of *Tbx3* is observed and *Tbx3* expression is, at least partially, restored (Li et al., 2004). These results, in combination with our own, suggest that regulatory relationships between *Tbx3* and *Gli3* may exist broadly during embryogenesis.

Our data implicate *Gli3* in a genetic network that can influence limb position, yet mice mutant for *Gli3* (*Extra toes*, *Xt*^{J}), are not reported to exhibit any shift in axial limb position (Buscher et al., 1997; Buscher et al., 1998; Hui and Joyner, 1993; Litingtung et al., 2002). In *Xt*^{J}/*Xt*^{J} mice (that lack all Gli3 activity), *dHand* is expressed throughout the limb and subsequently *Shh* is expressed ectopically in the anterior limb mesenchyme. Misexpression of *dHand* alone, at limb bud stages, is capable of inducing *Shh* expression, but only in the anterior limb mesenchyme rather than medial locations (Charite et al., 2000; Fernandez-Teran et al., 2000). These results suggest that anterior and posterior limb mesenchyme may express a 'licensing factor' required together with *dHand* for the induction of *Shh* and that this factor is absent from the medial limb mesenchyme. *Tbx3* is expressed in two stripes in the anterior and posterior limb mesenchyme at later stages of limb development (Fig. 1D) and may normally act as such a factor.

A requirement for *Tbx3* to establish or re-set the domain of *Shh*-expressing cells in the ZPA may also explain why no limb shift phenotype is observed in *Xt*^{J}/*Xt*^{J} mice. *Tbx3* expression is not expanded in *Xt*^{J}/*Xt*^{J} mice (Tumpel et al., 2002). Without the presence of both *Tbx3* and *dHand*, the position of the limb is not altered. In *Tbx3* misexpression experiments, however, *Tbx3* can repress *Gli3* and this leads to an expansion of *dHand*. The co-expression of *Tbx3* and *dHand* can, in turn, 'license' ectopic *Shh* expression, which, in turn, alters the position of the limb (Fig. 7).

Mice in which *Tbx3* is inactivated and humans with UMS who are haploinsufficient for *TBX3* are not reported to exhibit any shift in axial limb position. This is consistent with the model we propose for the role of *Tbx3* in the early limb bud. Although a limb shift phenotype is not observed in *Tbx3*$^{-/-}$ mice, the expression domains of *dHand* and *Shh* are downregulated or even eliminated (Davenport et al., 2003), consistent with *Tbx3* being required for their normal expression. This finding supports our conclusions that, although not strictly required to fix limb position, *Tbx3* is an important component of the signals establishing the position of the domain of *Shh*-expressing cells that comprise the ZPA in the posterior limb.

References

Agarwal, P., Wylie, J. N., Galceran, J., Arkhitko, O., Li, C., Deng, C., Grosschedl, R. and Bruneau, B. G. (2003). Tbx5 is essential for forelimb bud initiation following patterning of the limb field in the mouse embryo. *Development* **130**, 623-633.

Agulnik, S. I., Garvey, N., Hancock, S., Ruvinsky, I., Chapman, D. L., Agulnik, I., Bollag, R., Papaioannou, V. and Silver, L. M. (1996). Evolution of mouse T-box genes by tandem duplication and cluster dispersion. *Genetics* **144**, 249-254.

Ahn, D. G., Kourakis, M. J., Rohde, L. A., Silver, L. M. and Ho, R. K. (2002). T-box gene tbx5 is essential for formation of the pectoral limb bud. *Nature* **417**, 754-758.

Bai, C. B., Stephen, D. and Joyner, A. L. (2004). All mouse ventral spinal cord patterning by hedgehog is Gli dependent and involves an activator function of Gli3. *Dev. Cell* **6**, 103-115.

Bamshad, M., Lin, R. C., Law, D. J., Watkins, W. C., Krakowiak, P. A., Moore, M. E., Franceschini, P., Lala, R., Holmes, L. B., Gebuhr, T. C. et al. (1997). Mutations in human TBX3 alter limb, apocrine and genital development in ulnar-mammary syndrome. *Nat. Genet.* **16**, 311-315.

Burke, A. C. (2000). Hox genes and the global patterning of the somitic mesoderm. *Curr. Top. Dev. Biol.* **47**, 155-181.

Burke, A. C., Nelson, C. E., Morgan, B. A. and Tabin, C. (1995). Hox genes and the evolution of vertebrate axial morphology. *Development* **121**, 333-346.

Buscher, D., Bosse, B., Heymer, J. and Ruther, U. (1997). Evidence for genetic control of Sonic hedgehog by Gli3 in mouse limb development. *Mech. Dev.* **62**, 175-182.

Buscher, D., Grotewold, L. and Ruther, U. (1998). The XtJ allele generates a Gli3 fusion transcript. *Mamm. Genome* **9**, 676-678.

Carlson, H., Ota, S., Campbell, C. E. and Hurlin, P. J. (2001). A dominant repression domain in Tbx3 mediates transcriptional repression and cell immortalization: relevance to mutations in Tbx3 that cause ulnar-mammary syndrome. *Hum. Mol. Genet.* **10**, 2403-2413.

Charite, J., McFadden, D. G. and Olson, E. N. (2000). The bHLH transcription factor dHAND controls Sonic hedgehog expression and establishment of the zone of polarizing activity during limb development. *Development* **127**, 2461-2470.

Cohn, M. J., Izpisua-Belmonte, J. C., Abud, H., Heath, J. K. and Tickle, C. (1995). Fibroblast growth factors induce additional limb development from the flank of chick embryos. *Cell* **80**, 739-746.

Cohn, M. J., Patel, K., Krumlauf, R., Wilkinson, D. G., Clarke, J. D. and Tickle, C. (1997). Hox9 genes and vertebrate limb specification. *Nature* **387**, 97-101.

Dai, Y. S. and Cserjesi, P. (2002). The basic helix-loop-helix factor, HAND2, functions as a transcriptional activator by binding to E-boxes as a heterodimer. *J. Biol. Chem.* **277**, 12604-12612.

Dai, Y. S., Cserjesi, P., Markham, B. E. and Molkentin, J. D. (2002). The transcription factors GATA4 and dHAND physically interact to synergistically activate cardiac gene expression through a p300-dependent mechanism. *J. Biol. Chem.* **277**, 24390-24398.

Davenport, T. G., Jerome-Majewska, L. A. and Papaioannou, V. E. (2003). Mammary gland, limb and yolk sac defects in mice lacking Tbx3, the gene mutated in human ulnar mammary syndrome. *Development* **130**, 2263-2273.

Dietrich, S., Abou-Rebyeh, F., Brohmann, H., Bladt, F., Sonnenberg-Riethmacher, E., Yamaai, T., Lumsden, A., Brand-Saberi, B. and Birchmeier, C. (1999). The role of SF/HGF and c-Met in the development of skeletal muscle. *Development* **126**, 1621-1629.

Fernandez-Teran, M., Piedra, M. E., Kathiriya, I. S., Srivastava, D., Rodriguez-Rey, J. C. and Ros, M. A. (2000). Role of dHAND in the anterior-posterior polarization of the limb bud: implications for the Sonic hedgehog pathway. *Development* **127**, 2133-2142.

Francis, P. H., Richardson, M. K., Brickell, P. M. and Tickle, C. (1994). Bone morphogenetic proteins and a signalling pathway that controls patterning in the developing chick limb. *Development* **120**, 209-218.

Gibson-Brown, J. J., Agulnik, S. I., Silver, L. M., Niswander, L. and Papaioannou, V. E. (1998). Involvement of T-box genes Tbx2-Tbx5 in vertebrate limb specification and development. *Development* **125**, 2499-2509.

Hamburger, V. (1939). The development and innervation of transplanted limb primordia of chick embryos. *J. Exp. Zool.* **80**, 347-389.

Hamburger, V. and Hamilton, H. L. (1951). A series of normal stages in the development of the chick embryo. *J. Exp. Morphol.* **88**, 49-92.

Hui, C. C. and Joyner, A. L. (1993). A mouse model of greig cephalopolysyndactyly syndrome: the extra-toesJ mutation contains an intragenic deletion of the Gli3 gene. *Nat. Genet.* **3**, 241-246.

Jaynes, J. B. and O'Farrell, P. H. (1991). Active repression of transcription by the engrailed homeodomain protein. *EMBO J.* **10**, 1427-1433.

Jimenez, G., Paroush, Z. and Ish-Horowicz, D. (1997). Groucho acts as a corepressor for a subset of negative regulators, including Hairy and Engrailed. *Genes Dev.* **11**, 3072-3082.

Kardon, G. (1998). Muscle and tendon morphogenesis in the avian hind limb. *Development* **125**, 4019-4032.

Kawakami, Y., Capdevila, J., Buscher, D., Itoh, T., Rodriguez Esteban, C. and Izpisua Belmonte, J. C. (2001). WNT signals control FGF-dependent limb initiation and AER induction in the chick embryo. *Cell* **104**, 891-900.

Kispert, A., Koschorz, B. and Herrmann, B. G. (1995). The T protein encoded by Brachyury is a tissue-specific transcription factor. *EMBO J.* **14**, 4763-4772.

Li, Y., Zhang, H., Choi, S. C., Litingtung, Y. and Chiang, C. (2004). Sonic hedgehog signaling regulates Gli3 processing, mesenchymal proliferation, and differentiation during mouse lung organogenesis. *Dev. Biol.* **270**, 214-231.

Lillie, F. R. (1927). *The Development of the Chick*, 2nd edn. New York, NY: Holt.

Litingtung, Y., Dahn, R. D., Li, Y., Fallon, J. F. and Chiang, C. (2002). Shh and Gli3 are dispensable for limb skeleton formation but regulate digit number and identity. *Nature* **418**, 979-983.

Liu, C., Nakamura, E., Knezevic, V., Hunter, S., Thompson, K. and Mackem, S. (2003). A role for the mesenchymal T-box gene Brachyury in AER formation during limb development. *Development* **130**, 1327-1337.

Logan, M. and Tabin, C. (1998). Targeted gene misexpression in chick limb buds using avian replication-competent retroviruses. *Methods* **14**, 407-420.

Logan, M., Simon, H. G. and Tabin, C. (1998). Differential regulation of T-box and homeobox transcription factors suggests roles in controlling chick limb-type identity. *Development* **125**, 2825-2835.

Minguillon, C. and Logan, M. (2003). The comparative genomics of T-box genes. *Brief. Funct. Genom. Proteom.* **2**, 224-233.

Ng, J. K., Kawakami, Y., Buscher, D., Raya, A., Itoh, T., Koth, C. M., Esteban, C. R., Rodriguez-Leon, J., Garrity, D. M., Fishman, M. C. et al. (2002). The limb identity gene Tbx5 promotes limb initiation by interacting with Wnt2b and Fgf10. *Development* **129**, 5161-5170.

Ohashi, Y., Brickman, J. M., Furman, E., Middleton, B. and Carey, M. (1994). Modulating the potency of an activator in a yeast in vitro transcription system. *Mol. Cell. Biol.* **14**, 2731-2739.

Pourquie, O., Fan, C. M., Coltey, M., Hirsinger, E., Watanabe, Y., Breant, C., Francis-West, P., Brickell, P., Tessier-Lavigne, M. and le Douarin, N. M. (1996). Lateral and axial signals involved in avian somite patterning: a role for BMP4. *Cell* **84**, 461-471.

Rallis, C., Bruneau, B. G., del Buono, J., Seidman, C. E., Seidman, J. G., Nissim, S., Tabin, C. J. and Logan, M. P. (2003). Tbx5 is required for forelimb bud formation and continued outgrowth. *Development* **130**, 2741-2751.

Rancourt, D. E., Tsuzuki, T. and Capecchi, M. R. (1995). Genetic interaction between hoxb-5 and hoxb-6 is revealed by nonallelic noncomplementation. *Genes Dev.* **9**, 108-122.

Riddle, R. D., Johnson, R. L., Laufer, E. and Tabin, C. (1993). Sonic hedgehog mediates the polarizing activity of the ZPA. *Cell* **75**, 1401-1416.

Ruvinsky, I., Silver, L. M. and Gibson-Brown, J. J. (2000). Phylogenetic analysis of T-Box genes demonstrates the importance of amphioxus for understanding evolution of the vertebrate genome. *Genetics* **156**, 1249-1257.

Sasaki, H., Hui, C., Nakafuku, M. and Kondoh, H. (1997). A binding site for Gli proteins is essential for HNF-3beta floor plate enhancer activity in transgenics and can respond to Shh in vitro. *Development* **124**, 1313-1322.

Schlange, T., Arnold, H. H. and Brand, T. (2002). BMP2 is a positive regulator of Nodal signaling during left-right axis formation in the chicken embryo. *Development* **129**, 3421-3429.

Schweitzer, R., Vogan, K. J. and Tabin, C. J. (2000). Similar expression and regulation of Gli2 and Gli3 in the chick limb bud. *Mech. Dev.* **98**, 171-174.

Suzuki, T., Takeuchi, J., Koshiba-Takeuchi, K. and Ogura, T. (2004). Tbx Genes Specify Posterior Digit Identity through Shh and BMP Signaling. *Dev. Cell* **6**, 43-53.

Takeuchi, J. K., Koshiba-Takeuchi, K., Suzuki, T., Kamimura, M., Ogura, K. and Ogura, T. (2003). Tbx5 and Tbx4 trigger limb initiation through activation of the Wnt/Fgf signaling cascade. *Development* **130**, 2729-2739.

Tanaka, M. and Tickle, C. (2004). Tbx18 and boundary formation in chick somite and wing development. *Dev. Biol.* **268**, 470-480.

te Welscher, P., Fernandez-Teran, M., Ros, M. A. and Zeller, R. (2002). Mutual genetic antagonism involving GLI3 and dHAND prepatterns the vertebrate limb bud mesenchyme prior to SHH signaling. *Genes Dev.* **16**, 421-426.

Tumpel, S., Sanz-Ezquerro, J. J., Isaac, A., Eblaghie, M. C., Dobson, J.

and Tickle, C. (2002). Regulation of Tbx3 expression by anteroposterior signalling in vertebrate limb development. *Dev. Biol.* **250**, 251-262.

Vogel, A., Rodriguez, C. and Izpisua-Belmonte, J. C. (1996). Involvement of FGF-8 in initiation, outgrowth and patterning of the vertebrate limb. *Development* **122**, 1737-1750.

Wang, B., Fallon, J. F. and Beachy, P. A. (2000). Hedgehog-regulated processing of Gli3 produces an anterior/posterior repressor gradient in the developing vertebrate limb. *Cell* **100**, 423-434.

Williams, B. A. and Ordahl, C. P. (1994). Pax-3 expression in segmental mesoderm marks early stages in myogenic cell specification. *Development* **120**, 785-796.

Wilson, V. and Conlon, F. L. (2002). The T-box family. *Genome Biol.* **3**, REVIEWS3008.

Zuniga, A. and Zeller, R. (1999). Gli3 (Xt) and formin (ld) participate in the positioning of the polarising region and control of posterior limb-bud identity. *Development* **126**, 13-21.